NEUROSCIENCE
RESEARCH ARTICLE

Azam Asgarihafshejani et al. / Neuroscience 414 (2019) 141–153

Cell-Genotype Specific Effects of Mecp2 Mutation on Spontaneous and Nicotinic Acetylcholine Receptor-Evoked Currents in Medial Prefrontal Cortical Pyramidal Neurons in Female Rett Model Mice

Azam Asgarihafshejani, Raad Nashmi and Kerry R. Delaney*

Dept. of Biology, University of Victoria, Victoria, BC, Canada V8W2Y2

Abstract—Rett syndrome (RTT) is a neurodevelopmental disorder caused by mutation in the X-linked MECP2 gene. Random X-inactivation produces a mosaic of mutant (MT) and wild-type (WT) neurons in female *Mecp2*+/– (*het)* mice. Many RTT symptoms are alleviated by increasing activity in medial prefrontal cortex (mPFC) in RTT model mice (Howell et al., 2017). Using a GFP-MeCP2 fusion protein to distinguish WT from MT pyramidal neurons in mPFC we found cell autonomous (cell genotype specific) and non-autonomous effects of MeCP2 deficiency on spontaneous excitatory/inhibitory balance, nicotinic acetylcholine receptor (nAChR) currents and evoked activity. MT Layer 5 and 6 (L5, L6) neurons of male *nulls*, and MT L6 of *het* mice had reduced spontaneous excitatory synaptic input compared to WT in wild-type male (*WTm*), female (*WTf*) and *het* mice. Inhibitory synaptic charge in MT L6 equaled WT in 2–4-month *het*s. At 6–7 months inhibitory charge in WT in *het* slices was increased compared to both MT in *het* and WT in *WTf*; however, in *het*s the excitatory/inhibitory charge ratio was still greater in WT compared to MT. nAChR currents were reduced in L6 of *null*s and MT L6 in *het* slices compared to WT neurons of *het*, *WTm* and *WTf.* At 2–4 months, ACh perfusion increased frequency of inhibitory currents to L6 neurons equally in all genotypes but increased excitatory inputs to MT and WT in *het*s less than WT in *WTf*s. Unexpectedly ACh perfusion evoked greater sustained IPSC and EPSC input to L5 neurons of *null*s compared to *WTm*.

Key words: MeCP2, Rett syndrome, nicotinic acetylcholine receptor, excitation/inhibition balance, medial prefrontal cortex, cell autonomous.

INTRODUCTION

Rett syndrome (RTT) is a severe autism-like disorder occurring at a frequency of one in 10,000–15,000 live female births (Burd et al., 1991). Mutations in methyl-CpG-binding protein 2 (MeCP2), which regulates chromatin organization and global gene transcription account for 95% of RTT cases (Amir et al., 1999; Wan et al., 1999). RTT is characterized by a spectrum of symptoms including severe motor, sensory, cognitive and autonomic deficiencies that manifest in the first year of postnatal development (Percy et al., 2010; Bhattacherjee et al., 2017) including stereotyped limb movements, dystonia, dyskinesia, progressive rigidity, and profound intellectual disability (Humphreys and Barrowman, 2016) and epileptic seizures are a co-morbidity in approximately 80% of 7–12-year-old RTT patients (Jian et al., 2007).

MeCP2 is expressed in all human tissues, but is particularly highly expressed within neurons (Lewis et al., 1992; Tate et al., 1996). In the central nervous system, MeCP2 is expressed at low levels at first, but increases during neuronal maturation and synaptogenesis reaching its peak in post-migratory neurons, suggesting a role for MeCP2 in maintaining neuronal maturation, plasticity and activity (Cohen et al., 2003; Jung et al., 2003). Due to random X chromosome inactivation female heterozygous (*het*) RTT patients are mosaic, with approximately half of cells expressing the mutant *MECP2* allele, while the others express the normal. Loss of MeCP2 function in *het* RTT model mice has been reported to have both cell autonomous effects (specific to the MeCP2 status of the neuron) and cell non-autonomous effects (affecting cells that express mutant or non-mutant MeCP2) (Kishi and Macklis, 2010; Gantz et al., 2011; Rietveld et al., 2015). The heterogeneity of neuronal genotype within the *MECP2*+/– brain presents

*Corresponding author at: Dept. of Biology, University of Victoria, Victoria, BC, Canada V8W2Y2 Tel.: +1 250 472 5657.
E-mail address: kdelaney@uvic.ca (Kerry R. Delaney).

Abbreviations: 4*, alpha 4 subunit containing; excitatory, E; EPSC, excitatory postsynaptic current; *het*, heterozygous; inhibitory, I; IPSC, inhibitory postsynaptic current; L6, layer 6; mPFC, medial prefrontal cortex; MeCP2, methyl-CpG-binding protein 2; MT, mutant; nAChR, nicotinic acetylcholine receptor; Rett syndrome, RTT; WT, wild-type; WT-GFP, wild-type MeCP2 fused to GFP; *WTf*, wild-type female; *WTm*, wild-type male.

https://doi.org/10.1016/j.neuroscience.2019.07.008
0306-4522/

challenges for developing therapies and requires studies to include neuronal MeCP2 status when characterizing circuit function and responses to pharmacological and other interventions.

A growing body of evidence is revealing that the balance of excitation to inhibition (E/I) is changed, up or down, by loss of MeCP2 in a variety of brain regions including medial prefrontal cortex (mPFC), somatosensory cortex, hippocampus and brainstem (Dani et al., 2005; Li et al., 2016; Sceniak et al., 2016; Xu and Pozzo-Miller, 2017). Many aspects of neurochemistry are altered in RTT, including levels of neurotrophic factors and neuromodulatory systems (Zoghbi et al., 1989; Chang et al., 2006; Chao et al., 2010; Zhang et al., 2010; Durand et al., 2012; Kron et al., 2014; Oginsky et al., 2014; Li et al., 2016). Cholinergic (acetylcholine) transmission is known to be compromised in RTT patients. Although RTT is not a neurodegenerative disorder, fewer detectable choline acetyltransferase positive cells in basal forebrain (Wenk and Hauss-Wegrzyniak, 1999) and a reduction in choline acetyltransferase in hippocampus and thalamus (Wenk, 1997) have been reported. Studies have suggested that expression of several sub-types of nicotinic acetylcholine receptor (nAChR) mRNA is altered by MeCP2 mutation (Oginsky et al., 2014; Leung et al., 2017) and patients with a CHRNA5 (α5 nAChR subunit gene) mutation have been diagnosed with an RTT-like phenotype (Lucariello et al., 2016). Leung et al. (2017) identified nicotinic-dependent differences in locomotor behavior wherein injection of nicotinic agonists produced increased, rather than the normal decreased locomotor activity in MeCP2-null and has a reduced inhibitory effect on locomotion in symptomatic female mice. In mouse models loss of MeCP2 targeted to cholinergic neurons results in a partial RTT phenotype (Zhang et al., 2016). On the other hand, choline supplementation decreases some of the behavioral and neurobiological abnormalities of the RTT phenotype (Ward et al., 2009; Ricceri et al., 2011) possibly by enhancing NGF and BDNF expression in cortical regions as seen in cortical cultures (Johansson et al., 2009). Increased availability of choline during neurogenesis and synaptogenesis increases hippocampal dendritic spine density and ACh tissue content and permanently affects ACh turnover (Blusztajn, 1998; Jones et al., 1999). Selective restoration of MeCP2 in cholinergic neurons is sufficient to reverse locomotor impairments and decrease anxiety-like behaviors in RTT mice at least in early symptomatic stages, supporting future development of therapies associated with the cholinergic system (Kerr et al., 2012; Zhou et al., 2017).

ACh can affect a neuron directly, through postsynaptic receptors, or indirectly by presynaptically enhancing inhibitory or excitatory transmitter release and it is considered to be an essential modulator for complex cognitive functions such as learning, memory and attention as well as regulating locomotor motivation and coordination (Picciotto et al., 2012). mPFC is a part of the associational cortex, prominently implicated in attention deficit disorder and reduced nAChR sensitivity specific to mPFC has been demonstrated in an ADD mouse model, possibly due to changes in the subunit composition of α4 receptors (Tian et al., 2014). Attention deficit is one of the early symptoms of RTT that appear in infants (Parikh et al., 2007). Hypofunction in mPFC in RTT model mice has recently been shown to contribute to many symptoms of the disorder (Sceniak et al., 2016; Howell et al., 2017). mPFC is significantly modulated by nAChRs and the developmental profile of this modulation and description of cortical layer specific differences in nAChR subtype expression have been reported (Parikh et al., 2007; Alves et al., 2010; Klinkenberg et al., 2011; Poorthuis et al., 2013b; Tian et al., 2014). Recently nicotine treatment has been shown to relieve PFC hypofunction in a mouse model of addiction and schizophrenia (Koukouli et al., 2017).

We aim to understand the consequences of MeCP2 loss-of-function on nAChR-mediated transmission in the female *het* (*Mecp2*+/–) and male *null* (*Mecp2*–/*y*) CNS in areas including mPFC for which cholinergic dysfunction could contribute to the motor and attentional deficits of RTT. Our goal is to evaluate how lack of functional MeCP2 alters circuit function in the mPFC with particular focus on *het* females with their mosaic of neurons expressing either mutant (MT) or wild-type (WT) MeCP2. In *het* brains how does the presence of neurons with non-functional MeCP2 in mPFC affect basal activity and neuromodulation by nAChRs and does it differentially affect MT and WT neurons?

EXPERIMENTAL PROCEDURES

Animals

Experimental protocols were approved by the Animal Care Committee at the University of Victoria and all experiments were performed in accordance with guidelines from the Canadian Council of Animal Care. *Mecp2* mutant mice (*Mecp2*$^{tm1.1Jae}$/Mmcd) (MMRRC, UC Davis) (Jaenisch) were maintained on a C57BL/6 background. Although strictly not a null mutation since a truncated MeCP2 protein lacking the DNA binding region is produced in small quantities we refer to male *Mecp2*$^{-}$/*Y* mice as "*null*" for purposes of this study. Female *Mecp2*+/− heterozygotes (*het*) were crossed with male *GFP-Mecp2*$^{+}$/*Y* (*WTm*) mice (*Mecp2*-$^{tm3.1}$Bird/J, Jackson Laboratories) which express wild-type MeCP2 fused to GFP. Resultant *Mecp2*+/– offspring were produced in which cells expressing wild-type MeCP2 were labeled with green nuclei and mutant nuclei were without fluorescent label. Steroid hormones have been reported to alter nicotinic receptor function directly through allosteric modulation of α4β2* (* indicating that there may be other nACR subunits in the receptor) nicotinic receptors (Bertrand et al., 1991; Valera et al., 1992). Progestin binding sites are concentrated in cortical layer 6 (L6) suggesting that progesterone receptors are expressed in the deeper layers of cortex (Shughrue et al., 1991, 1992) so we used female mice in diestrus phase to reduce possible variability in responses.

47 female mice (30 wild-type and 17 *het*) and 50 male mice (19 *null* and 31 wild-type) were deeply anesthetized with isofluorane and decapitated for electrophysiological recording. The genotype of all animals resulting from

crosses of *het* females with males wild-type for *Mecp2* was confirmed by PCR after completion of physiological recording. At 6–8 weeks all the male *null* mice used for this study exhibited pronounced hindlimb and sometimes forelimb clasping when held by the tail, were hesitant in their locomotion, displayed a typically crouched posture and scruffy fur so that genotyping although undertaken was redundant. Visual assessment of females at 2–4 months was usually not readily predictive of genotype although slight hindlimb clasping was often observed. At >6 months moderate symptoms including pronounced hindlimb and forelimb clasping, ambulatory deficits (slight rolling gait) and sometimes weight gain were seen. Genotyping was performed on ear notches after completion of successful recordings.

Electrophysiology

Prefrontal coronal cortical slices (310 μm) were prepared from adult mice (male 6–8 weeks and female 2–7 months in diestrus stage). After transcardial perfusion with 25–30 ml of room temperature carbogenated (95% O_2/5% CO_2) N-Methyl-D-glucamine-based slicing solution containing (in mM): 92 NMDG, 2.5 KCl, 1.25 NaH2PO4, 30 NaHCO3, 20 Hepes, 25 D-glucose, 5 sodium ascorbate, 3 sodium pyruvate, 0.5 CaCl2, and 10 MgSO4 (pH 7.4 and 290–300 mOsm), prefrontal slices were cut (Leica 1000S, Concord, Canada) from anterior to posterior using the appearance of white matter and the corpus callosum as anterior and posterior land marks to target recording to medial prelimbic region. Slices were incubated for 30 min at room temperature in aCSF (125 mM NaCl, 10 mM D-glucose, 26 mM NaHCO3, 2 mM CaCl2, 1 mM MgSO4, 2.5 mM KCl, 1.25 mM NaH2PO4, myo-inositol 3 mM pH 7.4 and 290–300 mOsm). Slices were transferred to the recording chamber (Warner Instrument) and perfused with 31–33 °C carbogenated (95% O_2/5% CO_2) standard aCSF (2–3 ml/min).

Whole-cell voltage clamp recordings were obtained from pyramidal neurons in layer 5 or 6 of mPFC visualized by an Olympus BX51WI microscope. Recording pipettes (filamented borosilicate capillary glass 1.5 mm O.D. and 0.86 mm I.D., Sutter, USA) had tip resistances between 5 and 7 MΩ and were filled with pipette solution containing (in mM): 135 CsMeSO3, 5.5 CsCl, 5 QX-314-Cl, 10 HEPES, 10 Na-phosphocreatine, 2 MgATP and 0.3 NaGTP, 0.5 EGTA. The pH was set to 7.3–7.4 titrating with 1 M CsOH and the osmolarity adjusted to 290–300 mOsm.

MT and WT neurons were compared with respect to 1) spontaneous synaptic activity, 2) nAChR currents evoked by brief puffs of ACh (1 mM for 1 s) and 3) the effect of nAChR activity on excitatory and inhibitory synaptic inputs by continuous application of ACh (1 mM for 1 min).

WT and MT neurons were identified in *het* slices by the presence or absence of MeCP2-GFP, after recording to avoid bias. By recording from MT and WT neurons located in the same local area in *het* slices, sequentially and sometimes simultaneously, we tested the hypothesis that effects of MeCP2 on nAChR-mediated transmission are predominantly cell autonomous. The drug applicator system utilized low volume, solenoid controlled valves (Lee Co., Charlotte NC) and a theta tube that can rapidly switch between perfusing ACSF or agonist in less than 0.3 ms as measured by 10–90% rise time of a change in junction potential (see Komal et al., 2011) for description of rapid drug delivery apparatus). ACh was preferred to nicotine for these studies since it is removed by endogenous acetylcholinesterase and washes out more rapidly so is less prone to persistently desensitize receptors. To evoke direct nAChR-mediated currents, ACh was applied using 1-s, localized, rapid onset/offset puffs in the presence of atropine (200 nM) to block muscarinic AChRs. Repeated puff applications were separated by >2 min while holding at the Cl- reversal potential (≈ −75 mV).

Spontaneous and nAChR-evoked EPSCs and IPSCs were evaluated by holding at either the Cl- or GluR current reversal potentials (−75 or − 10 mV). Bicuculine was applied in several control experiments to verify the isolation of EPSCs or IPSCs at these holding potentials. The membrane potential was corrected for liquid junction potential (11 mV) and series resistance was monitored throughout the experiment. 50 μM 2-amino-5-phosphonovaleric acid (APV), 20 μM 6, 7-dinitroquinoxaline-2, 3-dione (DNQX), 20 μM bicuculine and 10 nM methyllycaconitine (α7nAChR antagonist), were used in some experiments.

Statistical analysis

Spontaneous and ACh-evoked EPSCs and IPSCs were analyzed using MiniAnalysis™ (Synaptosoft). Statistics were calculated using GraphPad Prism 6 or Social Sciences Calculator (https://www.socscistatistics.com/tests/). Statistical significance was determined using unpaired Student's T-test (within-group comparison of unpaired events) after confirming normalcy (Kolgoromov) and Tukey's multiple comparisons test to evaluate the criterion for statistical significance. Between one and seven cells (usually three or four) were sampled in each animal from left and/or right hemispheres of one or two sequential slices. All data in figures are presented as mean ± SEM of the number of cells. The number of cells and the number of animals from which the slices were obtained are indicated as cells (animals) in the figures and in the figure legends. Statistical comparisons based on the number of cells, and the average value for the cells in each animal are included in the text. Data sets which did not pass normalcy tests were evaluated non-parametrically. Symbols representing significance thresholds for figures are $P < 0.05$ (*), $P < 0.01$ (**), and $P < 0.001$ (***).

RESULTS

Experiments were undertaken in prelimbic area of mPFC to characterize spontaneous excitatory (E) and inhibitory (I) synaptic input, direct nAChR evoked currents and modulation of synaptic input by nAChR activation. For these studies we used puff and continuous application of ACh. We obtained recordings from L5 and L6 pyramids in *Mecp2*$^{+}$/*Y* (*WTm*) and *Mecp2*$^{-}$/Y (*null*) male slices. In female slices we recorded

from neurons expressing wild-type MeCP2 (WT) and mutant MeCP2 (MT) in *Mecp2*$^{+/-}$ (*het)* slices and compared these to WT neurons in *Mecp2*$^{+/+}$ (*WTf*) slices.

Male mice: Layer 6 pyramids

We recorded from L6 pyramids in 6–8 week old male slices to provide a comparison to measurements in *het* slices. L6 pyramidal neurons in *null* slices had significantly reduced spontaneous EPSC total charge compared to *WTm*, primarily due to a 31% reduction in the frequency of EPSCs (cells: t(98) = 3.16, P ≤ 0.01; animals t(25) =2.34, P < 0.05) (Fig. 1). IPSC frequency was higher in *null* slices (cells: t(43) = 4.05, P < 0.001; animals t(8) = 3.19, P = 0.01) resulting in a greater inhibitory charge assessed from the population of cells (t(43) = 2.14, P < 0.05), but not at the level of the small sample size for animals (t(8) = 1.67 P = 0.13). Overall there was a clear shift in the basal activity towards reduced excitation, due primarily to changes in spontaneous frequency of EPSCs and IPSCs. In this study our main focus was on neurons in female brains and due to a small sample size for which both E and I were

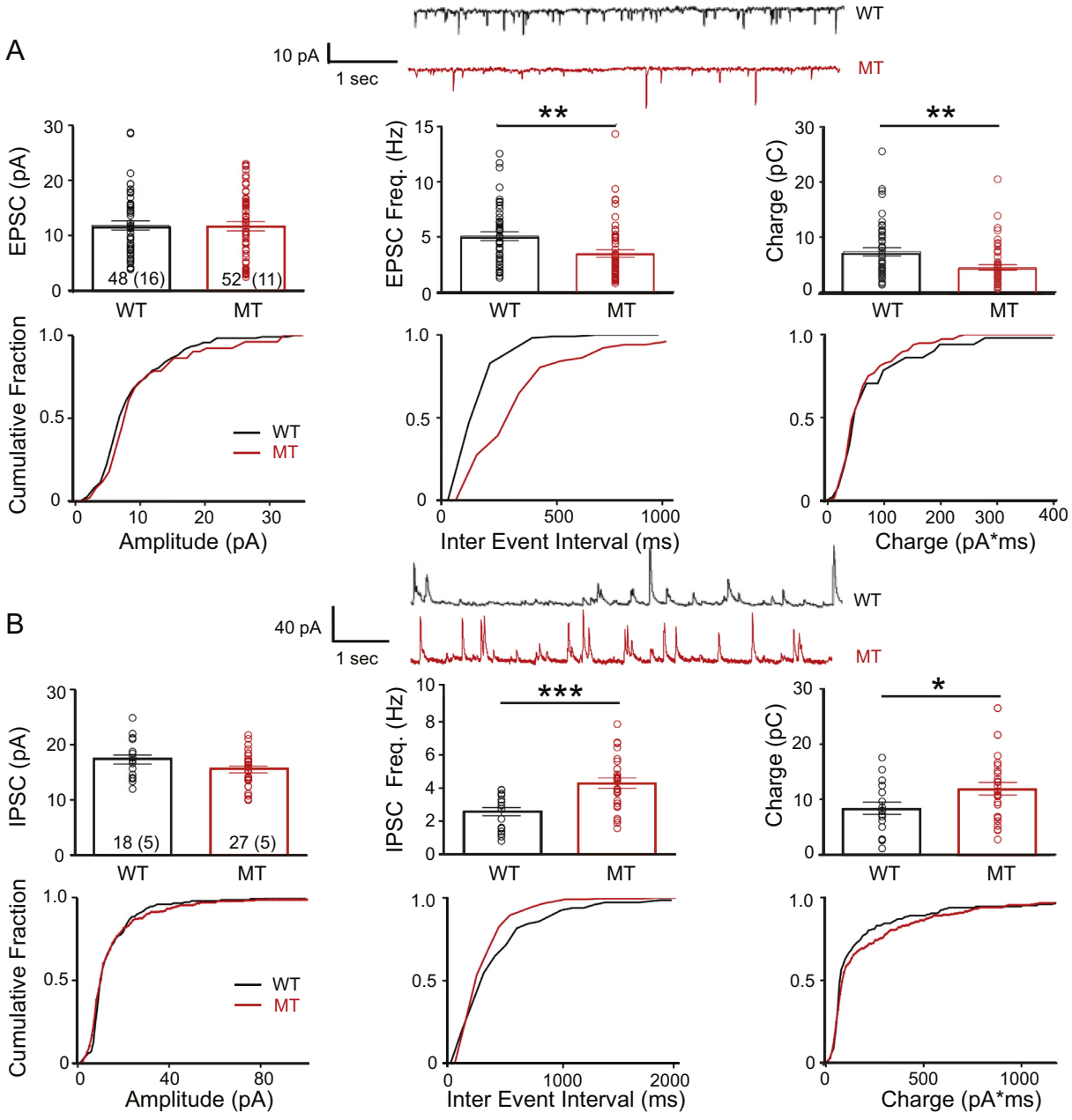

Fig. 1. WT vs. MeCP2-null male mice, spontaneous EPSCs and IPSCs in mPFC L6 pyramidal neurons. (**A)** Sample traces of EPSCs in WT (black) and null (MT; red), holding potential −75 mV. Charge calculated as the summed current over 60 s of recording. (WT EPSC, *n* = 48(16); *null* EPSC n = 52(11); WT IPSC *n* = 18 (5); *null* IPSC *n* = 27 (5)). Net EPSC charge and frequency are decreased 39% and 31% respectively MT compared to WT. (**B)** Sample recording of IPSCs in WT (black) and MT (red), holding potential +10 mV. IPSC frequency was 67% greater in MT vs WT (p ≤ 0.01; T-test). #(#) indicates number of cells and (animals), error bars are +/− SEM. (For interpretation of the references to color in this figure legend, the reader is referred to the web version of this article.)

obtained in the same male neurons a pairwise statistical evaluation of E/I ratio was not possible.

L6 pyramids express significant levels of α4* nAChR (Poorthuis et al., 2013b). Applying 1-s puffs of ACh directly to neurons in *null* slices we found AChR-currents were reduced 28% on average compared to non-GFP expressing neurons in *WTm* slices (cells: t(47) = 2.59, P < 0.05; animals t(8) = 2.20, P < 0.05). We also examined ACh-evoked currents in neurons expressing WT MeCP2 fused to GFP (WT-GFP) and found no difference compared to WT MeCP2 alone confirming a lack of effect of GFP fusion (t(26) = 0.98, P = 0.33). Including data from these three male animals expressing WT-GFP yields t(11) = 2.91, P < 0.01) (Fig. 2A). Currents were unaffected by application of the α7 antagonist methyllycaconitine (10 nM not shown).

Perfusing slices with 1 mM ACh we found the increase in the rate of spontaneous EPSCs was more sustained than for IPSCs. Although the spontaneous rate of IPSCs was higher in *null* slices, the increase during ACh application was similar to *WTm* (F (17,486) = 0.50, P = 0.95*)*. The spontaneous EPSC frequency in *null* slices was lower (as shown also in Fig. 1) but the initial change in frequency was similar to *WTm* although possibly less sustained over the duration of ACh application (F (17,486) = 0.36, P = 0.99). As a result the frequency of EPSCs in *null* slices did not attain levels similar to those in *WTm* and overall E to I balance remained lower in *null* vs *WTm.*

Female mice: Layer 6 pyramids

To examine the effect of MeCP2 loss of function in mPFC in female mice, we recorded from L6 pyramidal neurons of young *WTf* and pre- or mildly symptomatic (2–4 months) and older symptomatic (6–7 months) *het* slices (Fig. 3). L6 MT neurons of *hets* at both ages received significantly reduced spontaneous EPSC input compared to WT neurons in *het* slices, which was more evident at older ages. The frequency of inputs in MT compared to WT neurons

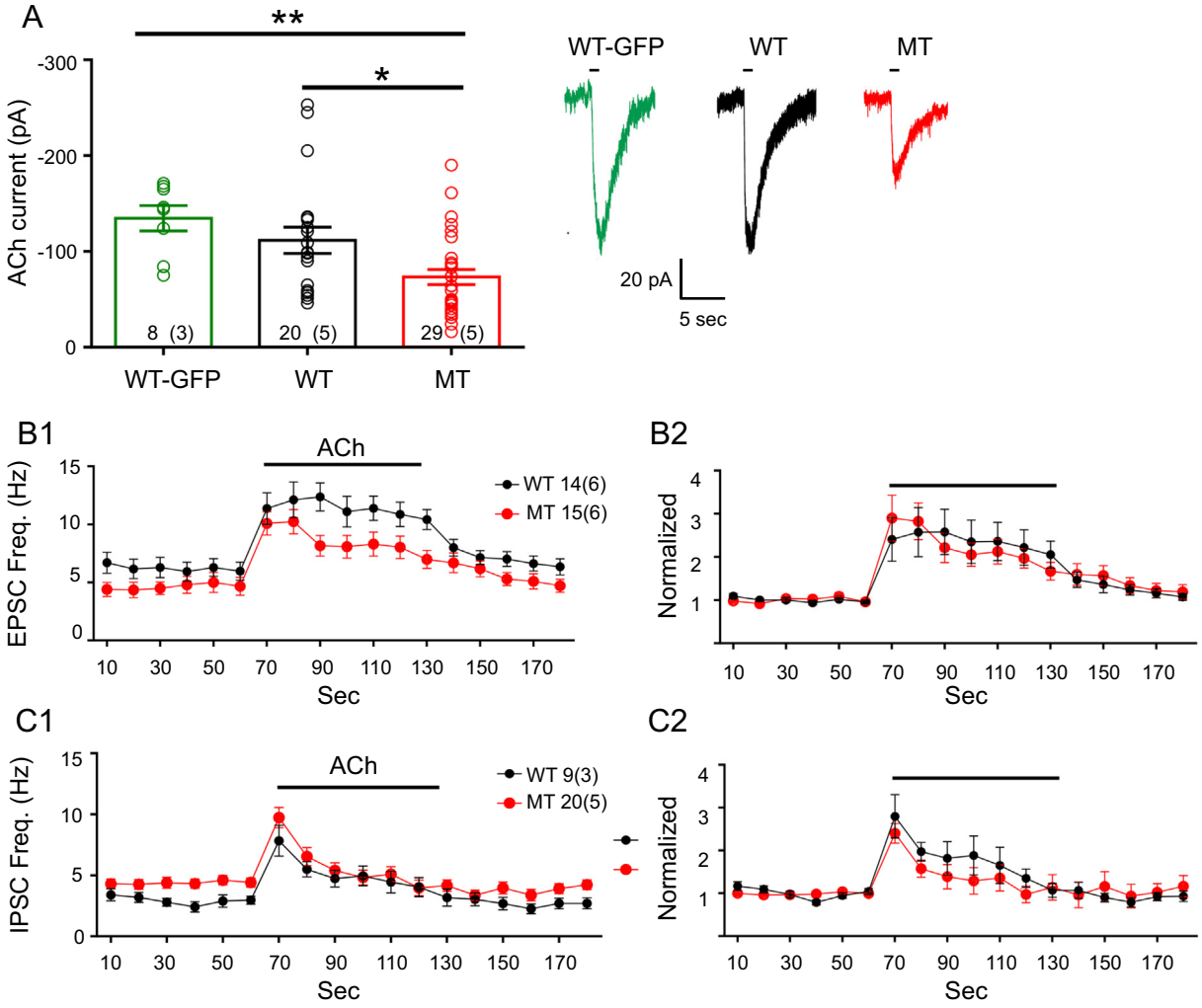

Fig. 2. Response to ACh of L6 pyramids mPFC of *Mecp2+/Y* (*WT*) and *Mecp2-/Y* (*MT*) slices. (**A)** 1-s puff of ACh to L6 evoked smaller nAChR-currents in MT neurons, *n* = 20(5) compared to WT MeCP2-GFP *n* = 8(3) and MeCP2 without GFP, *n* = 29(5). (**B)** Increased EPSC frequency during 1-min ACh application. Average increase in frequency for MT neurons is less than WT (4.2 vs 5.3 Hz, p ≤ 0.05, T-test) but normalizing to pre-ACh frequency reveals a proportionally equivalent increase for both genotypes (WT, *n* = 14(6); M, *n* = 15(6)). (**C)** No evidence for differential effect of ACh on increased rate of IPSC inputs (WT *n* = 9(3); MT, *n* = 20(5)). #(#) indicates number of cells and (animals), error bars are +/− SEM.

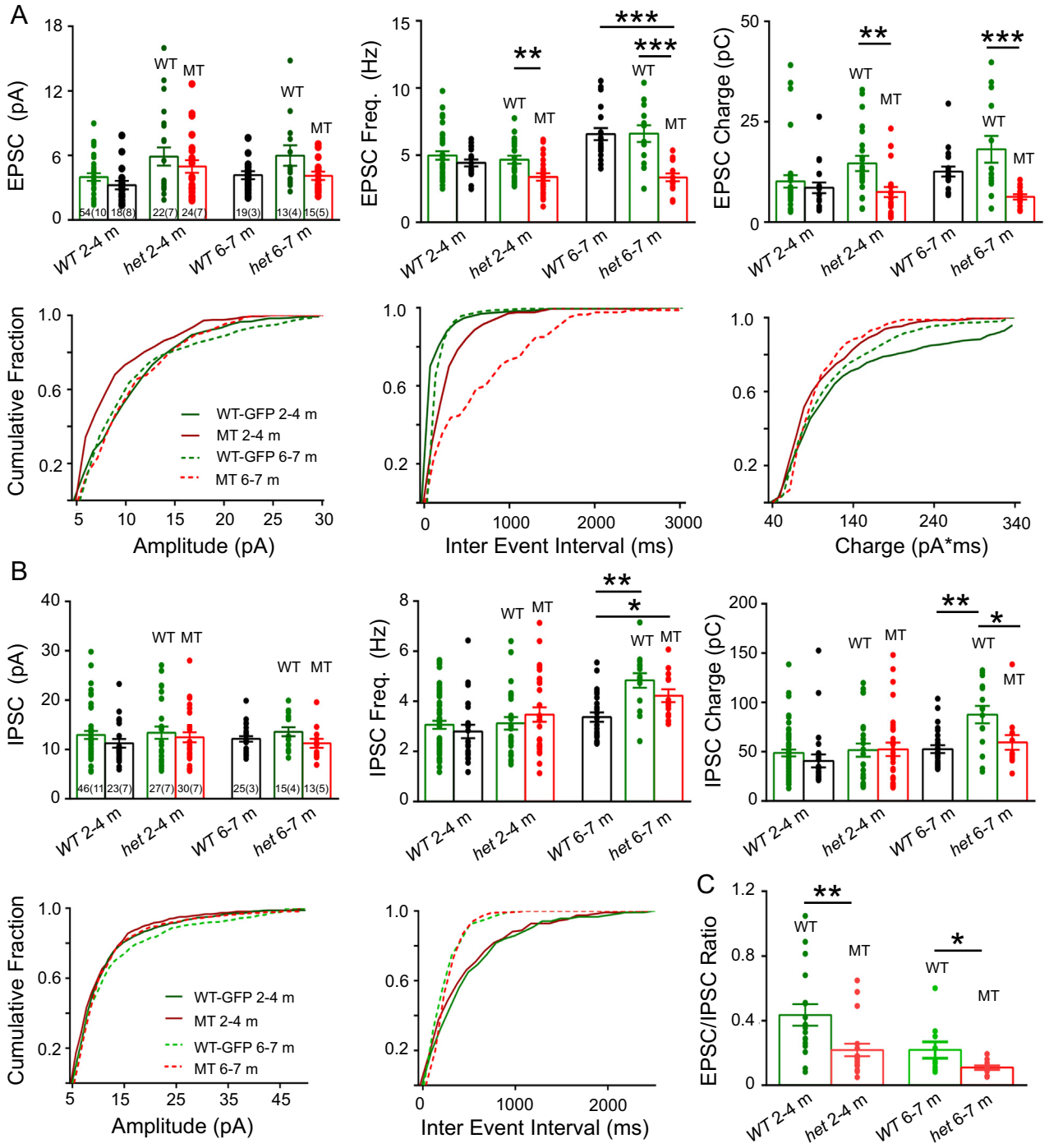

Fig. 3. Spontaneous EPSCs and IPSCs in mPFC layer 6 (L6) pyramidal neurons of female WT vs. *het* (*Mecp2*+/−) mice. (**A)** L6 MT pyramidal neurons of *het* mice exhibit significant reductions in spontaneous excitatory frequency and total charge compared to WT mice in both mildly symptomatic (2–4 months; WT n = 22(7); MT 24(7)) and symptomatic (6–7 months; WT n = 13(4), 15(5)) mice. For 2–4-month mice adjacent green and black bars are neurons in *WTf* mice expressing WT MeCP2-GFP and non-GFP neurons respectively. Adjacent green and red bars are neurons expressing WT-GFP and MT MeCP2 in *het* mice. For 6–7 months single black bar denotes neurons in *WTf* mice with non-GFP fused MeCP2. Adjacent green and red denote neurons in *het* mice expressing WT MeCP2-GFP and red is the MT neurons. (**B)** At 2–4 months no difference in IPSC frequency or total synaptic charge in neurons expressing MT, WT-GFP or WT MeCP2. At 6–7 months frequency is increased in both genotypes in *het* slices relative to *WTf* and for WT (n = 15(4)) compared to MT neurons (n = 13 (5) in *het* slices and WT neurons (n = 25(3) in *WTf* slices. (**C**) Ratio of excitatory charge to inhibitory charge is lower in MT versus WT neurons in *het* slices at both ages. Cumulative plots are single neurons representative of the average. #(#) indicates number of cells and (animals)), error bars are +/− SEM. (For interpretation of the references to color in this figure legend, the reader is referred to the web version of this article.)

was reduced compared to WT in *hets* (cells: F(2,44) =6.65, P < 0.001; animals: F(2,9) = 5.62, P < 0.01) and WT in *WTfs* (cells: F(2,44) = 7.23, P < 0.001; animals: F(2,9) 5.2, P < 0.01) (Fig. 3A). The difference in frequency, combined with a lack of difference in average EPSC amplitude resulted in a reduced excitatory charge which was somewhat more pronounced in older animals (2–4 months, cells: t(44) =3.18, P < 0.01; but animals: t(12) P > 0.05). At 6–7 months MT neurons received less spontaneous EPSC charge than WT (cells: F(2,44) = 3.52, P < 0.001; but animals: F(2,9), P > 0.05) and less than WT-GFP neurons (cells: F(2,44) = 6.04, P < 0.001; but animals F(2,9) = 3.47, P = 0.08) similar to MT neurons in symptomatic *null* males. At 2–4 months no difference was seen for IPSC amplitude, frequency or total charge between MT and WT neurons in *het*s. However, at 6–7 months the average frequencies of IPSCs in WT and MT neurons in *het* slices were statistically elevated compared to WT in *WTf* slices (Fig. 3B Tukeys multiple comparison F(2,50) = 8.53, P < 0.001) suggesting a more generalized cell non-autonomous effect of mutation as motor symptoms become established. Overall, IPSC total charge was reduced at 6–7 months in MT neurons compared to WT in *het* slices (cells: t(26) =2.37, P ≤ 0.05; animals: t(7) = 4.49, P < 0.01) although this appeared to be primarily due to greater increased IPSC activity in the WT neurons in *het* slices rather than a reduction in MT neurons. Comparing MT neurons in *het* slices to WT neurons in *WTf* slices we saw no difference while *WTf* neurons had less inhibitory charge than WT in *het* mice (t (38) = 4.11 P < 0.001) (Fig. 3B right panel). The net effect of *Mecp2* mutation is illustrated in panel 3C, which shows the E/I charge ratio for spontaneous synaptic inputs was significantly reduced at both ages in MT neurons compared to their WT counterparts in *het* slices (cells: t(34) =2.90, P ≤ 0.01 and t(21) =2.38, P < 0.05; animals: NS P > 0.05) (Fig. 3C). Overall these data indicate a reduction of spontaneous excitatory tone specific to neurons lacking functional MeCP2 in *het* animals (cell autonomous), which is more pronounced in older mice and development of hyperexcitability of spontaneous inhibitory activity in both MT and WT neurons.

We next examined the response to a 1-s puff of ACh to assess surface nAChR expression. In younger (2–4) and older (6–7 months) *het* slices we found reduced nAChR currents in MT compared to WT neurons (t(23) = 2.58 P < 0.05 and t(23) = 5.01, P < 0.001) (Fig. 4). In slices from 2–4-month *WTf* animals we also compared neurons expressing WT MeCP2-GFP fusion protein to neurons expressing WT MeCP2 and found no difference consistent with a lack of effect of the fusion of GFP to MeCP2 (t(44) = 0.10, P = 0.92). Limited numbers of animals were available for this study but currents were similar in average and distribution at both ages. Combining data from *hets* at the two ages supported a significant reduction in ACh current assessed across animals, (t(13) = 5.07, P < 0.001). Since currents in the WT cells in *hets* were similar to those in homozygous *WTf* animals at both ages the negative effect of mutation on nAChR sensitivity is primarily cell autonomous in L6 and restricted to the MT neurons.

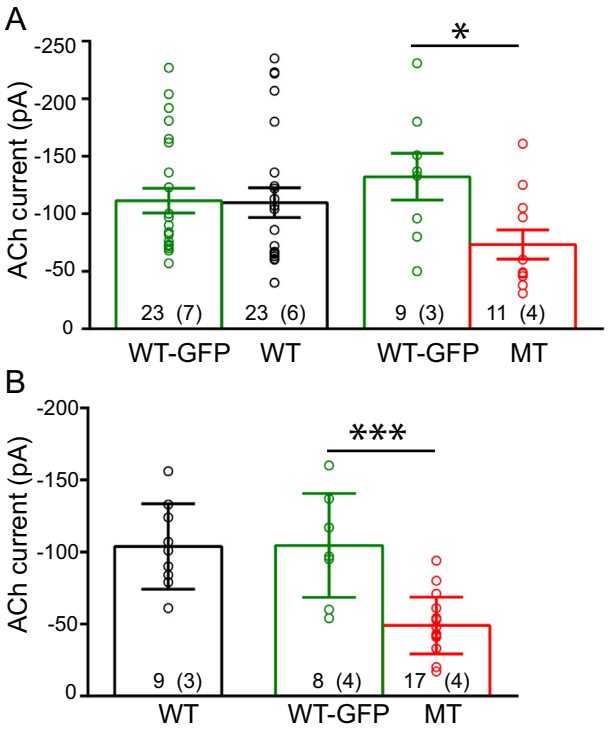

Fig. 4. One-second puff of 1 mM ACh to L6 mPFC pyramids in *WTf* and MT pyramids in *het* mice. (**A)** 2–4-month and (**B)** 6–7-month mice. For 2–4 months, adjacent green and black indicate WT (*n* = 23(7)) and WT-GFP neurons (*n* = 23(6) in *WTf* mice while adjacent green and red bars are WT-GFP (*n* = 11(4)) and MT MeCP2 (*n* = 8 (3) in *het* mice. For 6–7 months individual black bar denotes WT neurons in *WTf* mice, *n* = 9(3). Green bar is WT-GFP fusion neurons (*n* = 8(4)), red is MT, *n* = 17(4) in *het* mice. #(#) indicates number of cells (animals), error bars are +/− SEM. (For interpretation of the references to color in this figure legend, the reader is referred to the web version of this article.)

ACh was applied for 1 min to compare activation of EPSC and IPSCs into L6 neurons in slices from 2–4- and 6–7-month mice (Fig. 5). Since the basal frequency of PSCs differed between MT and WT neurons we assessed both the absolute and proportional effects for each genotype. ACh evoked a transient followed by a sustained increase in EPSCs. At 2–4 months the absolute, transient increase in EPSC frequency during the first 10 s was comparable for WT and MT neurons in *het* slices but lower than WT neurons in *WTf* slices (5–6 Hz, versus 10 Hz) suggesting an overall cell non-autonomous effect of lack of functional MeCP2 in half of neurons. The reduced activation combined with lower pre-ACh frequency resulted in a statistical difference for the MT neurons in *het* compared to WT in *WTf* slices (P < 0.05, Tukey's multiple comparison test).

Although smaller in amplitude the increased frequency in *het* slices was sustained during the 1-min application while tapering off more in *WTf* slices, so by about 30 s of perfusion frequencies were comparable in all neuron genotypes. Unexpectedly given the data for 2–4 month slices the increased frequency of EPSCs in MT and WT neurons in 6–7-month *het* slices were large and comparable to neurons in *WTf* slices so that ACh brought EPSC frequency in

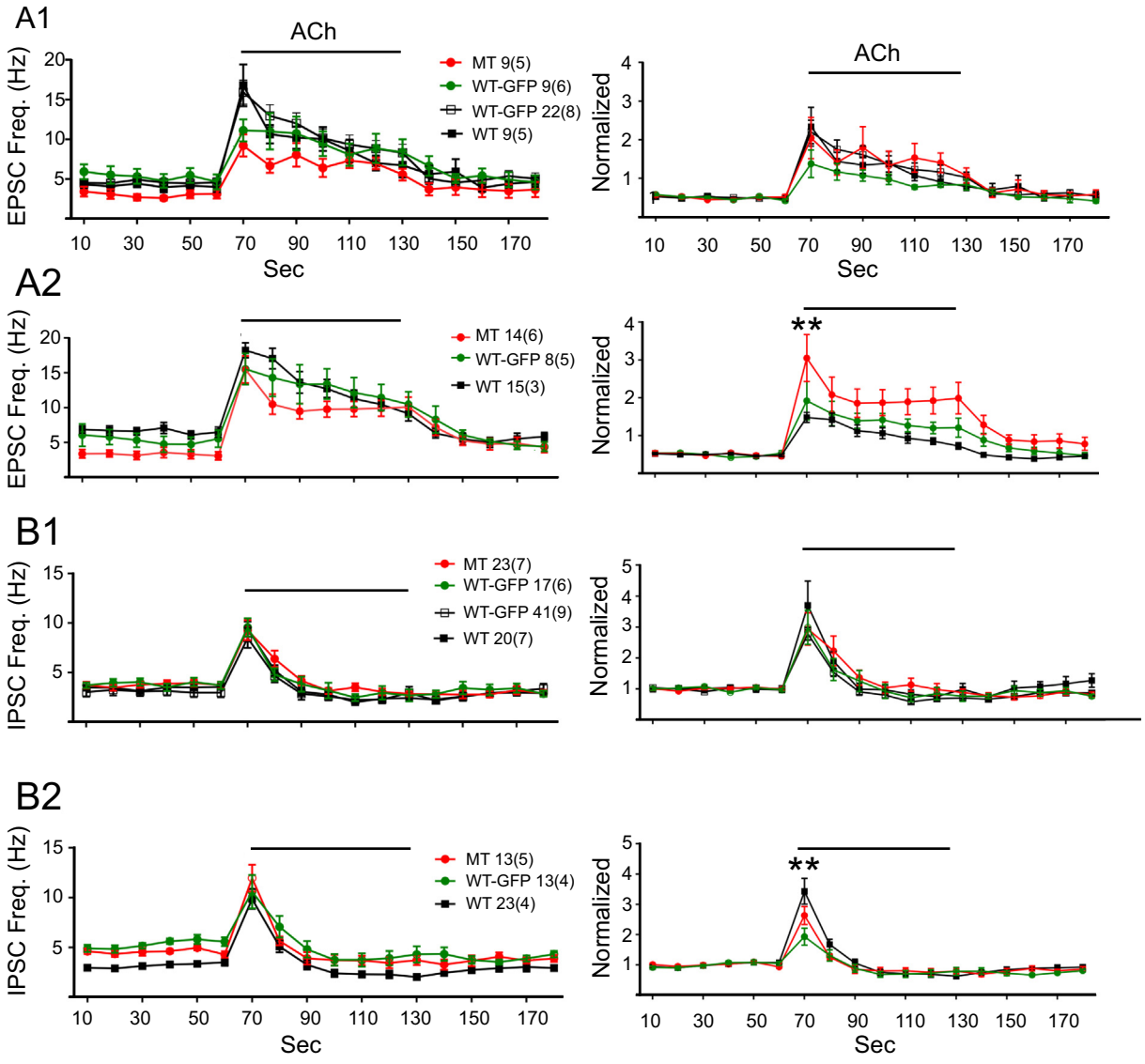

Fig. 5. ACh-evoked EPSCs and IPSCs into mPFC L6 pyramidal neurons in *WTf* versus *het* mice. **(A)** Frequency of EPSCs during 10-s intervals, A1 = 2–4-month slices, A2 = 6–7 months. Right panels are normalized frequency = f(t)/f(avg. 0–60 s). (**B**) Frequency of IPSCs during 10-s intervals, B1 = 2–4-month slices, B2 = 6–7 months. Green circles are WT-GFP and red circles are MT MeCP2, in *het* slices. Open black boxes at 2–4 months are WT-GFP neurons in *WTf* slices. At both ages filled black boxes are WT MeCP2 in *WTf* slices. #(#) on graphs indicates number of cells and (animals), error bars are +/− SEM. (For interpretation of the references to color in this figure legend, the reader is referred to the web version of this article.)

neurons in *het* slices to near those of *WTf* slices ($F(34,612) = 1.652$, $P \leq 0.01$).

The normalized increases in EPSC frequency are greatest for MT neurons at both ages due to their lower spontaneous pre-ACh frequency and inversely, lower for IPSCs (at 6–7 months) due to their higher spontaneous frequency pre-ACh. IPSC frequency increased to the same maximum, about 10 Hz, with a much more transient response than that of EPSCs followed by a slight net inhibition at both ages and cell genotypes ($F(34,828) = 2.29$, $P \leq 0.001$). For 6–7-month *het* slices the higher basal (pre-ACh) IPSC frequency resulted in a proportional increase that was least for the WT neurons about half that of the WT neurons of *WTf* slices.

In summary before development of clear motor symptoms activation of nAChRs has a less stimulatory effect on EPSC inputs to MT and WT L6 pyramids in *het* slices, which seems unaccompanied by increased activation of inhibitory inputs to these neurons.

Male mice: Layer 5 pyramids

Due to a shortage of *Mecp2* +/– mice we were only able to undertake studies of L5 MT versus WT neurons in male mice. With respect to L5 pyramids in *null* slices our results largely replicate Sceniak et al., (2016) with a reduction in spontaneous EPSC total charge (cells: $t(43) = 2.24$,

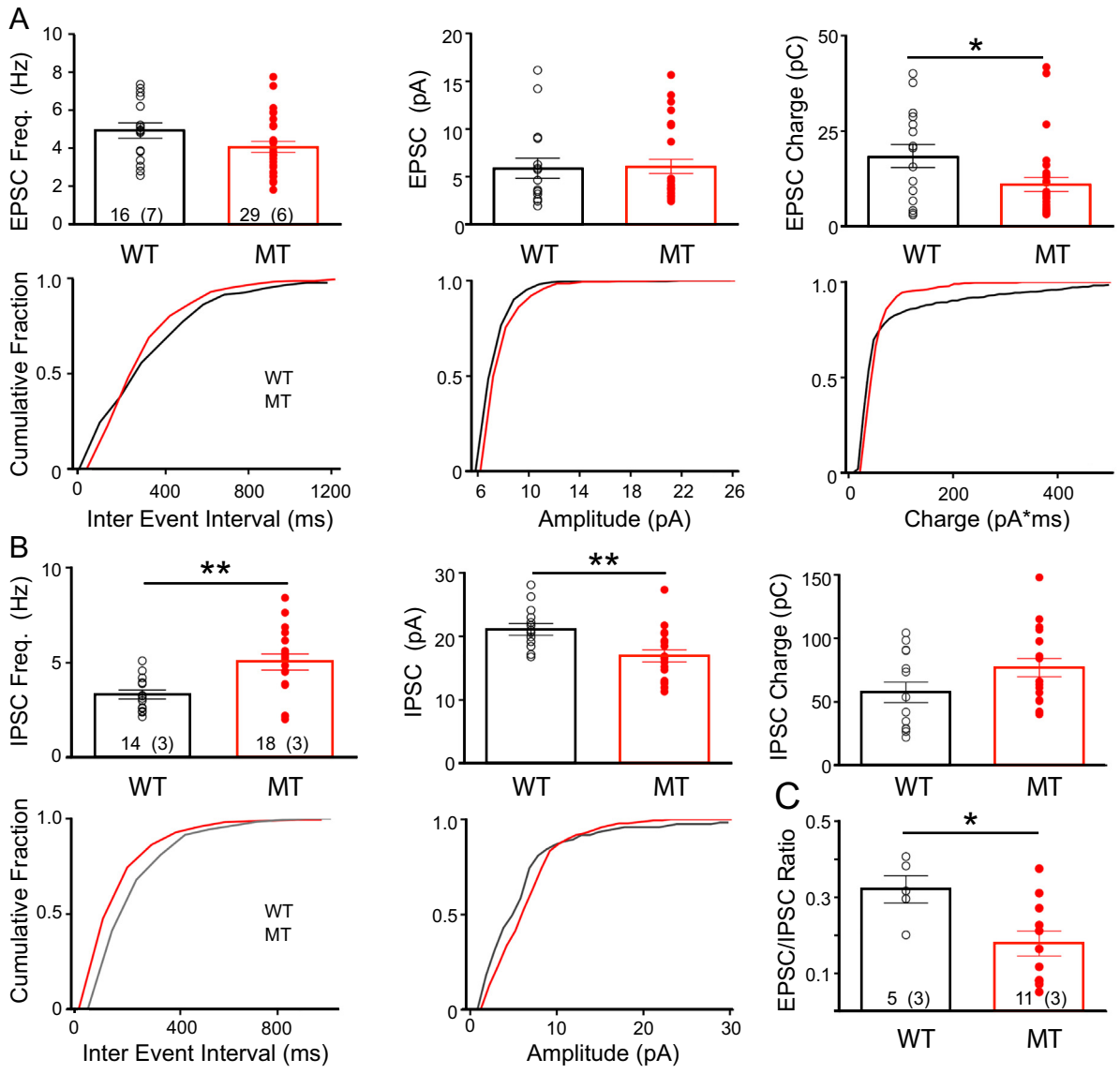

Fig. 6. Spontaneous EPSCs and IPSCs in L5 of mPFC pyramidal neurons in *WTm and null* (MT) mice. (**A)** There is a decrease in total excitatory current inputs to MT neurons (n = 16(7)) compared to WT (n = 29(6)) ($p < 0.05$; T- test). Cumulative distribution plots for single neurons representative of the average for amplitude, inter-event interval and charge. (**B**) Although there is a trend towards increased inhibition the pairwise calculated inhibitory synaptic charge was not statistically significantly different ($p = 0.08$; T-test) by virtue of offsetting differences in frequency ($p < 0.01$; T-test) and amplitude ($p < 0.01$; T-test) of inhibitory synaptic currents in MT (n = 18(3) compared to WT (n = 14(3). (**C)** Pairwise measurements of E and I charge reveal a significant decrease in the E/I charge ratio (n = 11(3). #(#) indicates number of cells and (animals), error bars are +/− SEM.

$P < 0.05$; animals $t(11) = 2.34$, $P < 0.05$) and an increase in inhibitory charge at the margin of statistical significance (Fig. 6B cells: $t(30) = 1.80$, $P = 0.08$). The opposing direction of changes in E and I charge for WT and MT neurons results in a 55% reduction of the average E charge divided by the average I charge for the entire population of cells sampled (Fig. 6 WT = 0.32, MT = 0.14). For the subset of 5 WT and 11 MT cells in which both E and I charges were measured the E/I charge ratio was significantly reduced in MT neurons ($t(14) = 2.59$, $P < 0.05$) by an amount equal to the average change in all cells (WT = 0.32, MT = 0.18, $p \leq 0.05$). Unfortunately the small sample size precluded a statistical comparison with reasonable power at the level of animals ($t(4) = 2.33$, $P = 0.08$). ACh evokes only small direct currents in L5 pyramids since they express few α4*nAChRs (Poorthuis et al., 2013a) and α7 receptors are not well activated by puff or continuous ACh in slices due to rapid desensitization. ACh application does however activate many E and I synaptic inputs ($F(17,506) = 1.74$, $P = 0.03$ and $F(17,648) = 2.85$, $P \leq 0.001$) (Fig. 7A, B), which are thought mainly to arise from generation of action potential dependent release from α4 expressing thalamic terminals (Heath et al., 2010). Unexpectedly ACh perfusion reliably increased IPSC and EPSC frequency more in MT versus WT neurons ($F(17,648) = 2.85$, $P < 0.001$) (Fig. 7B). The increased synaptic activity also persisted longer

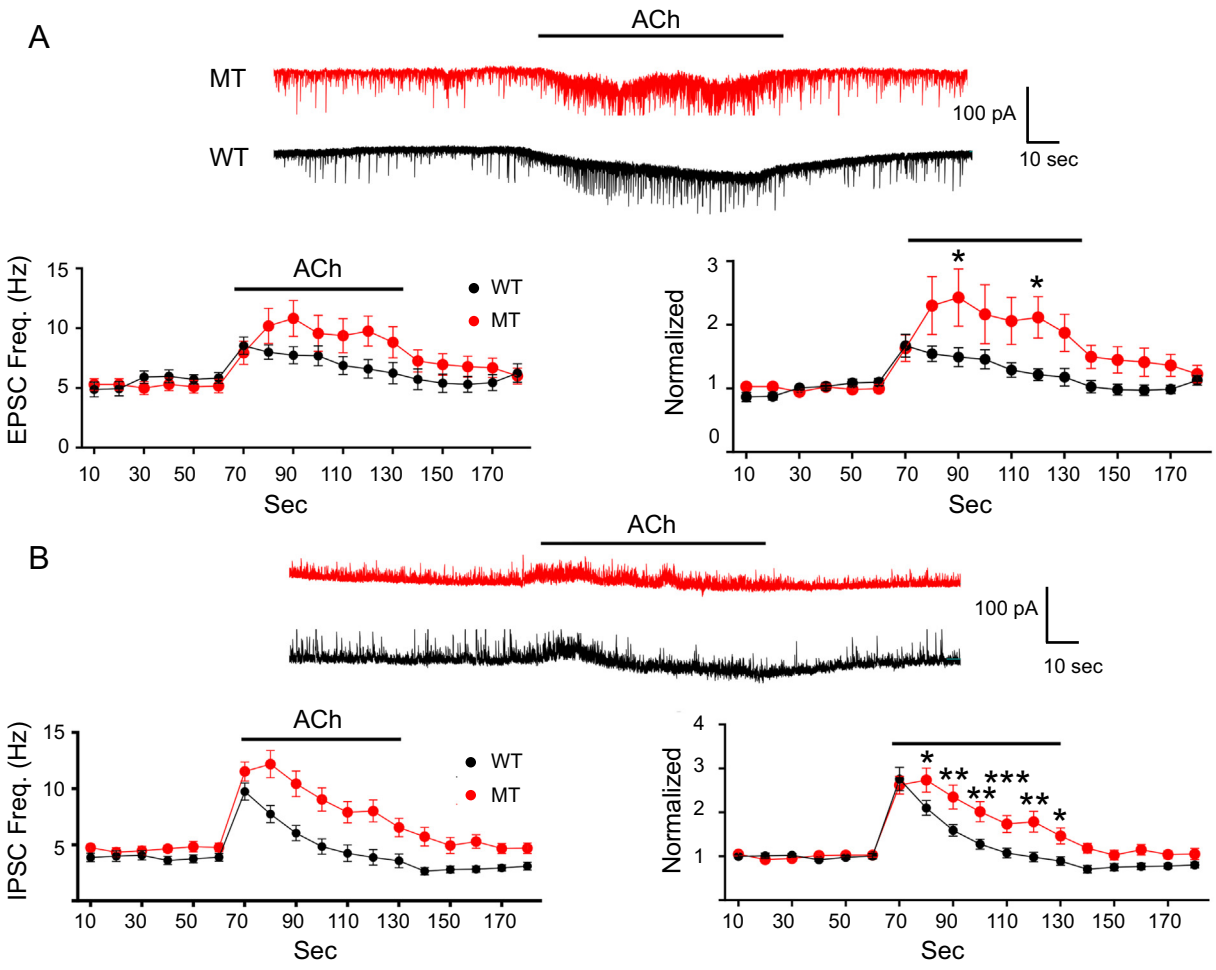

Fig. 7. ACh evoked synaptic inputs to male mPFC L5 pyramidal neurons, *WTm* and null (MT) mice. (**A)** Sample recording of EPSCs recorded at −75 mV for WT (black) and MT (red). Perfusion with ACh evokes only small direct nAChR currents in L5 pyramidal neurons but does however activate many EPSC synaptic inputs. Unexpectedly nAChR activation increased EPSC frequency significantly (Two-way ANOVA, Tukey's multiple comparisons test) and for a longer duration in MT vs. WT neurons. (**B)** Sample recording of IPSCs recorded at 10 mV for WT and null. 1-min ACh exposure activates many IPSCs. nAChR activation also increased IPSC frequency more (Two-way ANOVA, Tukey's test) and for a longer duration in MT vs. WT neurons. The mean inhibitory and excitatory synaptic inputs are shown for WT (cells: excitatory *n* = 16(4) and inhibitory *n* = 19(4)) versus MT neurons (excitatory *n* = 15(4) and inhibitory *n* = 19(5)). #(#) indicates number of cells and (animals), error bars are +/− SEM. (For interpretation of the references to color in this figure legend, the reader is referred to the web version of this article.)

than normal, most strikingly for IPSCs, which usually return to baseline rates within 20–30 s in WT L5 neurons but remained elevated during and for many seconds after washout.

DISCUSSION

Previous studies have indicated that primary sensory and motor neocortical circuits in MeCP2-null (male) mutant mouse models of RTT appear to be hypofunctional due to a shift in excitatory/inhibitory (E/I) synaptic balance (Dani et al., 2005; Dani and Nelson, 2009; Sceniak et al., 2016; Xu and Pozzo-Miller, 2017). Our findings show a loss of spontaneous excitatory tone and conserved or increased inhibitory input to mPFC pyramidal neurons lacking functional MeCP2 in male L5 and L6 and in L6 of *het* females. In *het* mPFC the reduction is specific to MT neurons and since WT neurons in the mosaic brain of *het* mice were in general similar to WT neurons in *WTf* mice the effect of lack of MeCP2 is definably cell autonomous to the deficient neuron and becomes evident before the appearance of overt motor systems suggesting an opportunity to intervene to address this developing imbalance before it increases and/or affects circuit development.

The specific reasons for E/I imbalance are not clear but reduction of glutamatergic excitatory drive, increased inhibitory connectivity, or a combination has been suggested (Dani et al., 2005; Dani and Nelson, 2009). Lee et al., (2008) proposed a relative immaturity in NMDA receptor subunit composition and function in *Mecp2* mutants in mPFC, consistent with a study that showed excitatory synaptic responses exhibited a reduction in ratio of NMDA/AMPA currents and reduced levels of NMDA receptor expression associated with altered network activity

(Sceniak et al., 2016). Our measurements did not discriminate between AMPA and NMDA but since EPCS were recorded at −75 mV holding potential they are unlikely to have much of an NMDAR-dependent component.

Rapid cholinergic signaling in the mPFC is essential for attention and is reduced in an attention deficit mouse model (Parikh et al., 2007; Sarter et al., 2009; Tian et al., 2014). Basal forebrain, cholinergic neuron lesions suggest a specific impact of ACh in attention, especially cholinergic projections to the prefrontal cortex (Pang et al., 1993; Voytko et al., 1994; Dalley et al., 2004; Newman and McGaughy, 2008). nAChRs impact mPFC through direct actions on neurons within the cortex and by modulating excitability and release from thalamic afferents. L6 pyramidal neurons and thalamic afferents to L5 express primarily α4*nAChRs. mPFC L6 is one of the few cortical regions and the only layer expressing the α5 nicotinic subunit (Wada et al., 1990; Marks et al., 1992; Salas et al., 2003; Heath et al., 2010). Inclusion of the α5 subunit alters several parameters of α4β2 nicotinic receptors including an increase in Ca^{+2} conductance (Brown et al., 2007; Tapia et al., 2007), increased sensitivity to nicotine and reduced desensitization to persistent nicotine application (Ramirez-Latorre et al., 1996). ACh-evoked currents in mPFC L6 pyramids were reduced by up to 50% in α5 KO mice (Tian et al., 2014). The reduced ACh-evoked current in MT L6 neurons (in *null* and *het*) might therefore arise from either fewer α4*nAChRs in general and/or a reduction in α4*α5nAChRs. The observation that reduced nAChR sensitivity and activation of excitatory inputs to L6 pyramids are developed as early as 2–4 months (although not as pronounced as at 6–7 months) suggests they are not a secondary cause of other changes related to the development of respiratory, seizure or motor symptoms. Thus this deficit, which is specific to MT L6 neurons, seems to differ from the reduction of D2 autoreceptors in substantia nigra, which is not seen until after symptoms are well-developed (Gantz et al., 2011).

Although the directly activated nAChR-evoked current in L6 pyramids is reduced at 2–4 and 6–7 months, the increased frequency of ACh-evoked EPSCs shows age/symptom level dependent differences. Increased basal activity in mPFC has been shown to have beneficial effects in MeCP2-deficient mice (Howell et al., 2017). Before the development of prominent motor symptoms bath application of ACh has reduced efficacy in both MT and WT neurons in *het* mice compared to *WTf*. Thus at least for L6 pyramids nAChR activation in *het* slices increases the ratio of E to I inputs to MT and WT neurons equally, likely because the presynaptic population comprises a mixture of MT and WT neurons and as such increases mPFC activity in a relatively balanced way. At 6–7 months the absolute increase in EPSC frequency of MT and WT neurons in *het* slices is greater than in 2–4 month slices, and similar to neurons in *WT* slices. Although MT neurons have low levels of spontaneous EPSCs inputs, during ACh application the frequency of inputs is essentially the same for MT and WT neurons and similar to neurons in *WTf* slices. The proportionately greater increase of EPSCs into MT neurons, combined with mostly similar effects on IPSCs helps to normalize the ratio of E to I activity during ACh application. This suggests that nAChRs may be a target to relieve mPFC hypofunction without creating additional imbalance in *het* brains.

In Leung et al., (2017) pre- and post-symptomatic females showed no difference in α4 mRNA expression in midbrain plus thalamus and only in 9–12 month, strongly symptomatic females, was α4 mRNA increased in cortical tissue. In this respect symptomatic females were similar to symptomatic males. Thus there is a mismatch between overall cortical α4mRNA expression and L6 neuron responses since direct ACh-evoked currents are reduced in MT neurons from pre- and postsymptomatic mice at ages when there is apparently either no change, or an increase in cortical α4 mRNA expression.

ACh evokes only a small direct nAChR current in L5 pyramids since they express few α4*nAChRs and the α7-type they do express is not efficiently activated by puff or continuous ACh in brain slices due to rapid desensitization. L5 receives thalamic inputs that are strongly modulated by α4*nAChRs (Lambe et al., 2003; Poorthuis et al., 2013b) but thalamic neurons do not express α5 subunits (Marks et al., 1992; Heath et al., 2010) so an increase in α4α5* receptors on thalamocortical terminals in male MeCP2-null mPFC is not likely to account for the increased and prolonged ACh-evoked EPSC and IPSCs. In symptomatic male *nulls* α4 (and α6) mRNA expression was reduced by >50% in the thalamus and midbrain but was increased by 50% in cortex (Leung et al., 2017). Thus the ACh-evoked responses in MT mPFC pyramids are opposite to α4 mRNA levels assessed at the level of brain regions: reduced direct currents in the L6 pyramidal neurons that express α4*nAChRs and increased activation of synaptic inputs to L5 pyramids, which are largely mediated by α4*nAChR bearing thalamocortical projections (Lambe et al., 2003) from midbrain where mRNA expression is apparently reduced. The increased nAChR sensitivity of inputs to L5 may reflect compensatory responses to reduced cholinergic tone and/or reduced activity in thalamocortical neurons. Since qRT-PCR was performed on the entire cortical tissue (see Leung et al., 2017), that study could not determine whether the 50% increase in α4 (and α6) mRNA expression in *het* females was limited to specific cortical layers or neuronal subtypes. Furthermore, mRNA expression may not directly correlate to protein expression. Therefore, knowledge of cell specific nAChR subunit protein expression differences would be potentially more informative of the mechanisms of the electrophysiological changes in MT cells.

In this respect the sustained increased IPSC frequency in L5 neurons in *null* slices during ACh application, compared to the transient response in *WTm*, warrants further study (in *nulls* and *hets*). It may reflect an alteration in the efficacy of frequency dependent disynaptic inhibition between L5 neurons (Naka and Adesnik, 2016; Obermayer et al., 2018), which is revealed when ACh activates mPFC circuits. Alternatively it may reflect reduced efficacy of ACh to activate vasoactive intestinal peptide expressing GABA neurons, which normally have an inhibitory effect on somatostatin and parvalbumin expressing GABA neurons that provide

inhibitory input to L5 pyramids (Bell et al., 2015; Wood et al., 2017; Morello et al., 2018).

ACKNOWLEDGMENTS

This work was supported by the International Rett Syndrome Foundation through a mentored postdoctoral fellowship to AA (3009) and operating grant to KD (3005), and by operating grants from the Natural Sciences and Engineering Research Council Canada to KD (RGPIN 2014-05950) and RN (RGPIN 2018-04581) and a Canadian Institutes of Health Research Project Grant to RN (PJT 159548).

DECLARATION OF INTERESTS

None.

REFERENCES

Alves NC, Bailey CD, Nashmi R, Lambe EK. (2010) Developmental sex differences in nicotinic currents of prefrontal layer VI neurons in mice and rats. PLoS One 5e9261.

Amir RE, Van den Veyver IB, Wan M, Tran CQ, Francke U, Zoghbi HY. (1999) Rett syndrome is caused by mutations in X-linked MECP2, encoding methyl-CpG-binding protein 2. Nat Genet 23:185-188.

Bell LA, Bell KA, McQuiston AR. (2015) Acetylcholine release in mouse hippocampal CA1 preferentially activates inhibitory-selective interneurons via alpha4beta2* nicotinic receptor activation. Front Cell Neurosci 9:115.

Bertrand D, Valera S, Bertrand S, Ballivet M, Rungger D. (1991) Steroids inhibit nicotinic acetylcholine receptors. Neuroreport 2:277-280.

Bhattacherjee A, Winter MK, Eggimann LS, Mu Y, Gunewardena S, Liao Z, Christianson JA, Smith PG. (2017) Motor, somatosensory, viscerosensory and metabolic impairments in a heterozygous female rat model of Rett syndrome. Int J Mol Sci 19.

Blusztajn JK. (1998) Choline, a vital amine. Science 281:794-795.

Brown RW, Collins AC, Lindstrom JM, Whiteaker P. (2007) Nicotinic alpha5 subunit deletion locally reduces high-affinity agonist activation without altering nicotinic receptor numbers. J Neurochem 103:204-215.

Burd L, Randall T, Martsolf JT, Kerbeshian J. (1991) Rett syndrome symptomatology of institutionalized adults with mental retardation: comparison of males and females. Am J Ment Retard 95:596-601.

Chang Q, Khare G, Dani V, Nelson S, Jaenisch R. (2006) The disease progression of Mecp2 mutant mice is affected by the level of BDNF expression. Neuron 49:341-348.

Chao HT, Chen H, Samaco RC, Xue M, Chahrour M, Yoo J, Neul JL, Gong S, Lu HC, Heintz N, Ekker M, Rubenstein JL, Noebels JL, Rosenmund C, Zoghbi HY. (2010) Dysfunction in GABA signalling mediates autism-like stereotypies and Rett syndrome phenotypes. Nature 468:263-269.

Cohen DR, Matarazzo V, Palmer AM, Tu Y, Jeon OH, Pevsner J, Ronnett GV. (2003) Expression of MeCP2 in olfactory receptor neurons is developmentally regulated and occurs before synaptogenesis. Mol Cell Neurosci 22:417-429.

Dalley JW, Theobald DE, Bouger P, Chudasama Y, Cardinal RN, Robbins TW. (2004) Cortical cholinergic function and deficits in visual attentional performance in rats following 192 IgG-saporin-induced lesions of the medial prefrontal cortex. Cereb Cortex 14:922-932.

Dani VS, Nelson SB. (2009) Intact long-term potentiation but reduced connectivity between neocortical layer 5 pyramidal neurons in a mouse model of Rett syndrome. J Neurosci 29:11263-11270.

Dani VS, Chang Q, Maffei A, Turrigiano GG, Jaenisch R, Nelson SB. (2005) Reduced cortical activity due to a shift in the balance between excitation and inhibition in a mouse model of Rett syndrome. Proc Natl Acad Sci U S A 102:12560-12565.

Durand S, Patrizi A, Quast KB, Hachigian L, Pavlyuk R, Saxena A, Carninci P, Hensch TK, Fagiolini M. (2012) NMDA receptor regulation prevents regression of visual cortical function in the absence of Mecp2. Neuron 76:1078-1090.

Gantz SC, Ford CP, Neve KA, Williams JT. (2011) Loss of Mecp2 in substantia nigra dopamine neurons compromises the nigrostriatal pathway. J Neurosci 31:12629-12637.

Heath CJ, King SL, Gotti C, Marks MJ, Picciotto MR. (2010) Corticothalamic connectivity is vulnerable to nicotine exposure during early postnatal development through alpha4/beta2/alpha5 nicotinic acetylcholine receptors. Neuropsychopharmacology 35:2324-2338.

Howell CJ, Sceniak MP, Lang M, Krakowiecki W, Abouelsoud FE, Lad SU, Yu H, Katz DM. (2017) Activation of the medial prefrontal cortex reverses cognitive and respiratory symptoms in a mouse model of Rett syndrome. eNeuro 4.

Humphreys P, Barrowman N. (2016) The incidence and evolution of parkinsonian rigidity in Rett syndrome: a pilot study. Can J Neurol Sci 43:567-573.

Jian L, Nagarajan L, de Klerk N, Ravine D, Christodoulou J, Leonard H. (2007) Seizures in Rett syndrome: an overview from a one-year calendar study. Eur J Paediatr Neurol 11:310-317.

Johansson J, Formaggio E, Fumagalli G, Chiamulera C. (2009) Choline up-regulates BDNF and down-regulates TrkB neurotrophin receptor in rat cortical cell culture. Neuroreport 20:828-832.

Jones JP, Meck WH, Williams CL, Wilson WA, Swartzwelder HS. (1999) Choline availability to the developing rat fetus alters adult hippocampal long-term potentiation. Brain Res Dev Brain Res 118:159-167.

Jung BP, Jugloff DG, Zhang G, Logan R, Brown S, Eubanks JH. (2003) The expression of methyl CpG binding factor MeCP2 correlates with cellular differentiation in the developing rat brain and in cultured cells. J Neurobiol 55:86-96.

Kerr B, Soto CJ, Saez M, Abrams A, Walz K, Young JI. (2012) Transgenic complementation of MeCP2 deficiency: phenotypic rescue of Mecp2-null mice by isoform-specific transgenes. Eur J Hum Genet 20:69-76.

Kishi N, Macklis JD. (2010) MeCP2 functions largely cell-autonomously, but also non-cell-autonomously, in neuronal maturation and dendritic arborization of cortical pyramidal neurons. Exp Neurol 222:51-58.

Klinkenberg I, Sambeth A, Blokland A. (2011) Acetylcholine and attention. Behav Brain Res 221:430-442.

Komal P, Evans G, Nashmi R. (2011) A rapid agonist application system for fast activation of ligand-gated ion channels. J Neurosci Methods 198:246-254.

Koukouli F, Rooy M, Tziotis D, Sailor KA, O'Neill HC, Levenga J, Witte M, Nilges M, Changeux JP, Hoeffer CA, Stitzel JA, Gutkin BS, DiGregorio DA, Maskos U. (2017) Nicotine reverses hypofrontality in animal models of addiction and schizophrenia. Nat Med 23:347-354.

Kron M, Lang M, Adams IT, Sceniak M, Longo F, Katz DM. (2014) A BDNF loop-domain mimetic acutely reverses spontaneous apneas and respiratory abnormalities during behavioral arousal in a mouse model of Rett syndrome. Dis Model Mech 7:1047-1055.

Lambe EK, Picciotto MR, Aghajanian GK. (2003) Nicotine induces glutamate release from thalamocortical terminals in prefrontal cortex. Neuropsychopharmacology 28:216-225.

Lee S, Kim W, Ham BJ, Chen W, Bear MF, Yoon BJ. (2008) Activity-dependent NR2B expression is mediated by MeCP2-dependent epigenetic regulation. Biochem Biophys Res Commun 377:930-934.

Leung J, McPhee DM, Renda A, Penty N, Farhoomand F, Nashmi R, Delaney KR. (2017) MeCP2-deficient mice have reduced alpha4 and alpha6 nicotinic receptor mRNA and altered behavioral response to nicotinic agonists. Behav Brain Res 330:118-126.

Lewis JD, Meehan RR, Henzel WJ, Maurer-Fogy I, Jeppesen P, Klein F, Bird A. (1992) Purification, sequence, and cellular localization of a novel chromosomal protein that binds to methylated DNA. Cell 69:905-914.

Li W, Xu X, Pozzo-Miller L. (2016) Excitatory synapses are stronger in the hippocampus of Rett syndrome mice due to altered synaptic trafficking of AMPA-type glutamate receptors. Proc Natl Acad Sci U S A 113:E1575-E1584.

Lucariello M, Vidal E, Vidal S, Saez M, Roa L, Huertas D, Pineda M, Dalfo E, Dopazo J, Jurado P, Armstrong J, Esteller M. (2016) Whole exome sequencing of Rett syndrome-like patients reveals the

mutational diversity of the clinical phenotype. Hum Genet 135:1343-1354.
Marks MJ, Pauly JR, Gross SD, Deneris ES, Hermans-Borgmeyer I, Heinemann SF, Collins AC. (1992) Nicotine binding and nicotinic receptor subunit RNA after chronic nicotine treatment. J Neurosci 12:2765-2784.
Morello N, Schina R, Pilotto F, Phillips M, Melani R, Plicato O, Pizzorusso T, Pozzo-Miller L, Giustetto M. (2018) Loss of Mecp2 causes atypical synaptic and molecular plasticity of parvalbumin-expressing interneurons reflecting Rett syndrome-like sensorimotor defects. eNeuro 5.
Naka A, Adesnik H. (2016) Inhibitory circuits in cortical layer 5. Front Neural Circuits 10:35.
Newman LA, McGaughy J. (2008) Cholinergic deafferentation of prefrontal cortex increases sensitivity to cross-modal distractors during a sustained attention task. J Neurosci 28:2642-2650.
Obermayer J, Heistek TS, Kerkhofs A, Goriounova NA, Kroon T, Baayen JC, Idema S, Testa-Silva G, Couey JJ, Mansvelder HD. (2018) Lateral inhibition by Martinotti interneurons is facilitated by cholinergic inputs in human and mouse neocortex. Nat Commun 9:4101.
Oginsky MF, Cui N, Zhong W, Johnson CM, Jiang C. (2014) Alterations in the cholinergic system of brain stem neurons in a mouse model of Rett syndrome. Am J Physiol Cell Physiol 307:C508-C520.
Pang K, Williams MJ, Egeth H, Olton DS. (1993) Nucleus basalis magnocellularis and attention: effects of muscimol infusions. Behav Neurosci 107:1031-1038.
Parikh V, Kozak R, Martinez V, Sarter M. (2007) Prefrontal acetylcholine release controls cue detection on multiple timescales. Neuron 56:141-154.
Percy AK, Neul JL, Glaze DG, Motil KJ, Skinner SA, Khwaja O, Lee HS, Lane JB, Barrish JO, Annese F, McNair L, Graham J, Barnes K. (2010) Rett syndrome diagnostic criteria: lessons from the natural history study. Ann Neurol 68:951-955.
Picciotto MR, Higley MJ, Mineur YS. (2012) Acetylcholine as a neuromodulator: cholinergic signaling shapes nervous system function and behavior. Neuron 76:116-129.
Poorthuis RB, Bloem B, Schak B, Wester J, de Kock CP, Mansvelder HD. (2013) Layer-specific modulation of the prefrontal cortex by nicotinic acetylcholine receptors. Cereb Cortex 23:148-161.
Poorthuis RB, Bloem B, Verhoog MB, Mansvelder HD. (2013) Layer-specific interference with cholinergic signaling in the prefrontal cortex by smoking concentrations of nicotine. J Neurosci 33:4843-4853.
Ramirez-Latorre J, Yu CR, Qu X, Perin F, Karlin A, Role L. (1996) Functional contributions of alpha5 subunit to neuronal acetylcholine receptor channels. Nature 380:347-351.
Ricceri L, De Filippis B, Fuso A, Laviola G. (2011) Cholinergic hypofunction in MeCP2-308 mice: beneficial neurobehavioural effects of neonatal choline supplementation. Behav Brain Res 221:623-629.
Rietveld L, Stuss DP, McPhee D, Delaney KR. (2015) Genotype-specific effects of Mecp2 loss-of-function on morphology of layer V pyramidal neurons in heterozygous female Rett syndrome model mice. Front Cell Neurosci 9:145.
Salas R, Orr-Urtreger A, Broide RS, Beaudet A, Paylor R, De Biasi M. (2003) The nicotinic acetylcholine receptor subunit alpha 5 mediates short-term effects of nicotine in vivo. Mol Pharmacol 63:1059-1066.
Sarter M, Parikh V, Howe WM. (2009) Phasic acetylcholine release and the volume transmission hypothesis: time to move on. Nat Rev Neurosci 10:383-390.
Sceniak MP, Lang M, Enomoto AC, James Howell C, Hermes DJ, Katz DM. (2016) Mechanisms of functional hypoconnectivity in the medial prefrontal cortex of Mecp2 null mice. Cereb Cortex 26:1938-1956.
Shughrue PJ, Stumpf WE, Elger W, Schulze PE, Sar M. (1991) Progestin receptor cells in mouse cerebral cortex during early postnatal development: a comparison with preoptic area and central hypothalamus using autoradiography with [125I]progestin. Brain Res Dev Brain Res 59:143-155.
Shughrue PJ, Sar M, Stumpf WE. (1992) Progestin target cell distribution in forebrain and midbrain regions of the 8-day postnatal mouse brain. Endocrinology 130:3650-3659.
Tapia L, Kuryatov A, Lindstrom J. (2007) Ca2+ permeability of the (alpha4)3(beta2)2 stoichiometry greatly exceeds that of (alpha4)2 (beta2)3 human acetylcholine receptors. Mol Pharmacol 71:769-776.
Tate P, Skarnes W, Bird A. (1996) The methyl-CpG binding protein MeCP2 is essential for embryonic development in the mouse. Nat Genet 12:205-208.
Tian MK, Bailey CD, Lambe EK. (2014) Cholinergic excitation in mouse primary vs. associative cortex: region-specific magnitude and receptor balance. Eur J Neurosci 40:2608-2618.
Valera S, Ballivet M, Bertrand D. (1992) Progesterone modulates a neuronal nicotinic acetylcholine receptor. Proc Natl Acad Sci U S A 89:9949-9953.
Voytko ML, Olton DS, Richardson RT, Gorman LK, Tobin JR, Price DL. (1994) Basal forebrain lesions in monkeys disrupt attention but not learning and memory. J Neurosci 14:167-186.
Wada E, McKinnon D, Heinemann S, Patrick J, Swanson LW. (1990) The distribution of mRNA encoded by a new member of the neuronal nicotinic acetylcholine receptor gene family (alpha 5) in the rat central nervous system. Brain Res 526:45-53.
Wan M, Lee SS, Zhang X, Houwink-Manville I, Song HR, Amir RE, Budden S, Naidu S, Pereira JL, Lo IF, Zoghbi HY, Schanen NC, Francke U. (1999) Rett syndrome and beyond: recurrent spontaneous and familial MECP2 mutations at CpG hotspots. Am J Hum Genet 65:1520-1529.
Wenk GL. (1997) Rett syndrome: neurobiological changes underlying specific symptoms. Prog Neurobiol 51:383-391.
Ward BC, Kolodny NH, Nag N, Berger-Sweeney JE. (2009) Neurochemical changes in a mouse model of Rett syndrome: changes over time and in response to perinatal choline nutritional supplementation. J Neurochem 108:361-371.
Wenk GL, Hauss-Wegrzyniak B. (1999) Altered cholinergic function in the basal forebrain of girls with Rett syndrome. Neuropediatrics 30:125-129.
Wood KC, Blackwell JM, Geffen MN. (2017) Cortical inhibitory interneurons control sensory processing. Curr Opin Neurobiol 46:200-207.
Xu X, Pozzo-Miller L. (2017) EEA1 restores homeostatic synaptic plasticity in hippocampal neurons from Rett syndrome mice. J Physiol 595:5699-5712.
Zhang X, Su J, Rojas A, Jiang C. (2010) Pontine norepinephrine defects in Mecp2-null mice involve deficient expression of dopamine beta-hydroxylase but not a loss of catecholaminergic neurons. Biochem Biophys Res Commun 394:285-290.
Zhang Y, Cao SX, Sun P, He HY, Yang CH, Chen XJ, Shen CJ, Wang XD, Chen Z, Berg DK, Duan S, Li XM. (2016) Loss of MeCP2 in cholinergic neurons causes part of RTT-like phenotypes via alpha7 receptor in hippocampus. Cell Res 26:728-742.
Zhou H, Wu W, Zhang Y, He H, Yuan Z, Zhu Z, Zhao Z. (2017) Selective preservation of cholinergic MeCP2 rescues specific Rett-syndrome-like phenotypes in MeCP2(stop) mice. Behav Brain Res 322:51-59.
Zoghbi HY, Milstien S, Butler IJ, Smith EO, Kaufman S, Glaze DG, Percy AK. (1989) Cerebrospinal fluid biogenic amines and biopterin in Rett syndrome. Ann Neurol 25:56-60.

(Received 17 January 2019, Accepted 1 July 2019)
(Available online 09 July 2019)